

Supplementary material

Figure S1. Minimum spanning network among partial COI haplotypes of *Profilicollis botulus*.

Figure S2. Rooted phylogenetic trees of *Profilicollis botulus* based on partial COI sequences.

Figure S3. Frequency distribution of crab host sizes of the three crab species.

Figure S4. Correlations of prevalences of acanthocephalan infections at 7 sampling locations.

Figure S5. Correlations of mean intensities of acanthocephalan infections at 7 sampling locations.

Figure S6. Frequency distribution of *Carcinus maenas* carapace sizes separated into males and females.

Figure S7. Prevalence of the rhizocephalan *Sacculina carcini* in *Carcinus maenas* crab hosts at the 10 sampling locations.

Recommended Citation of this material:

Goedknegt MA, Havermans J, Waser AM, Luttikhuisen PC, Velilla E, Camphuysen K, van der Meer J, Thieltges DW (2017) Cross-species comparison of parasite richness, prevalence, and intensity in a native compared to two invasive brachyuran crabs. *Aquatic Invasions* 12: 201–212, <https://doi.org/10.3391/ai.2017.12.2.08>

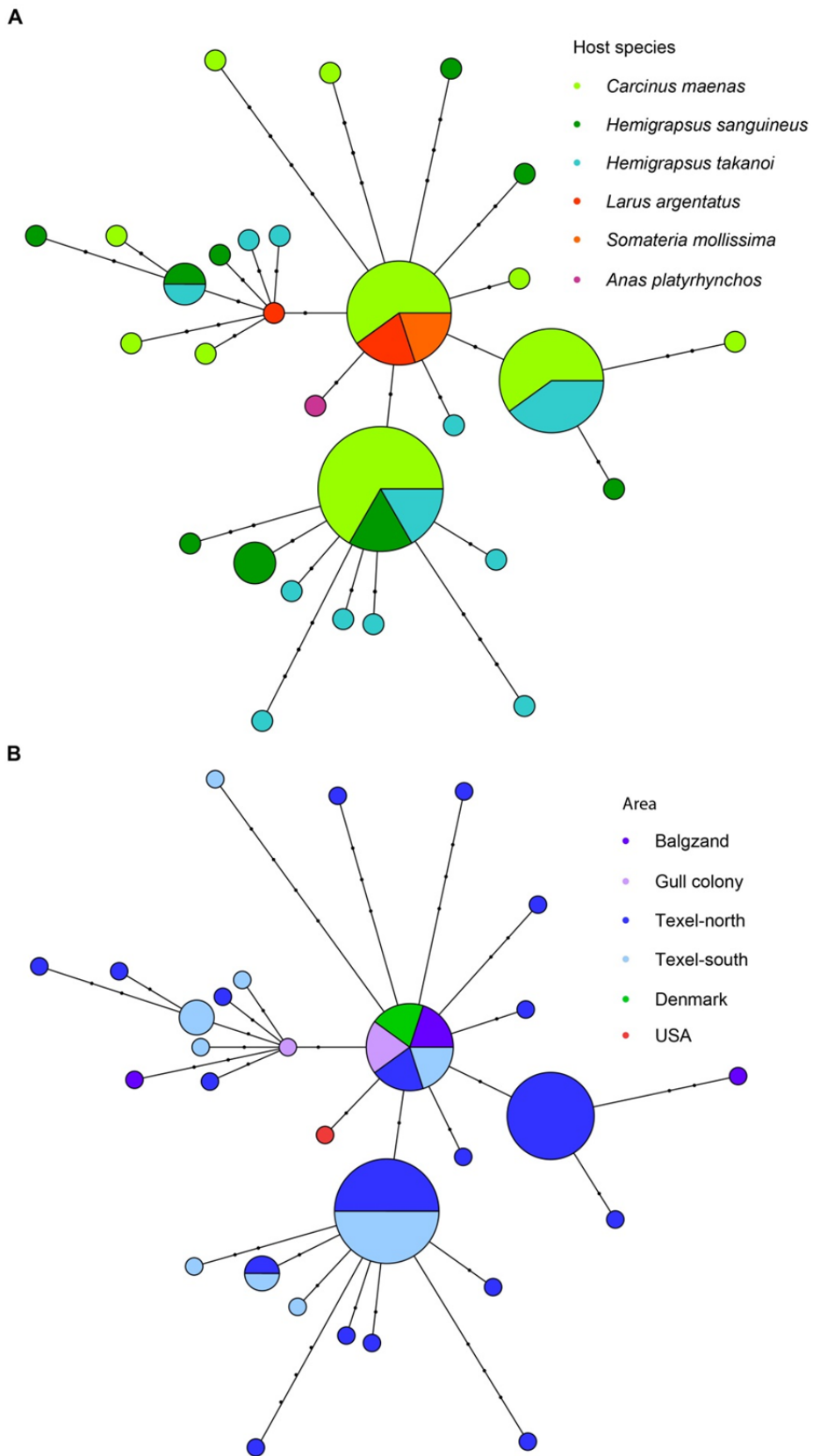


Figure S1. Minimum spanning network among partial cytochrome-c-oxidase I haplotypes of *Proflicollis botulus* in different A) host species and B) sampling areas.

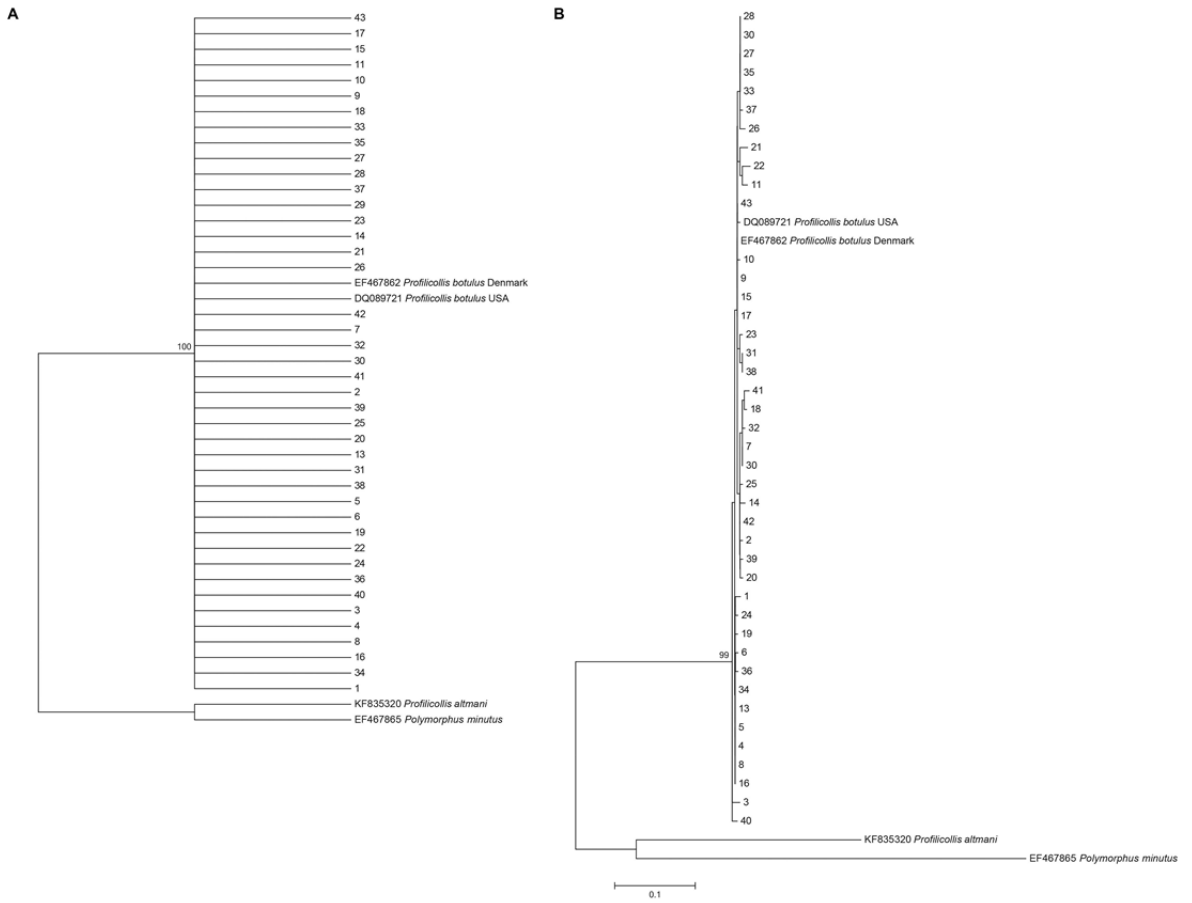


Figure S2. Rooted phylogenetic trees of *Profilocollis botulus* based on partial COI sequences. A) Maximum parsimony tree; B) Maximum likelihood tree. Values on trees are bootstrap values from 500 bootstrap replicates; values below 80% are not shown.

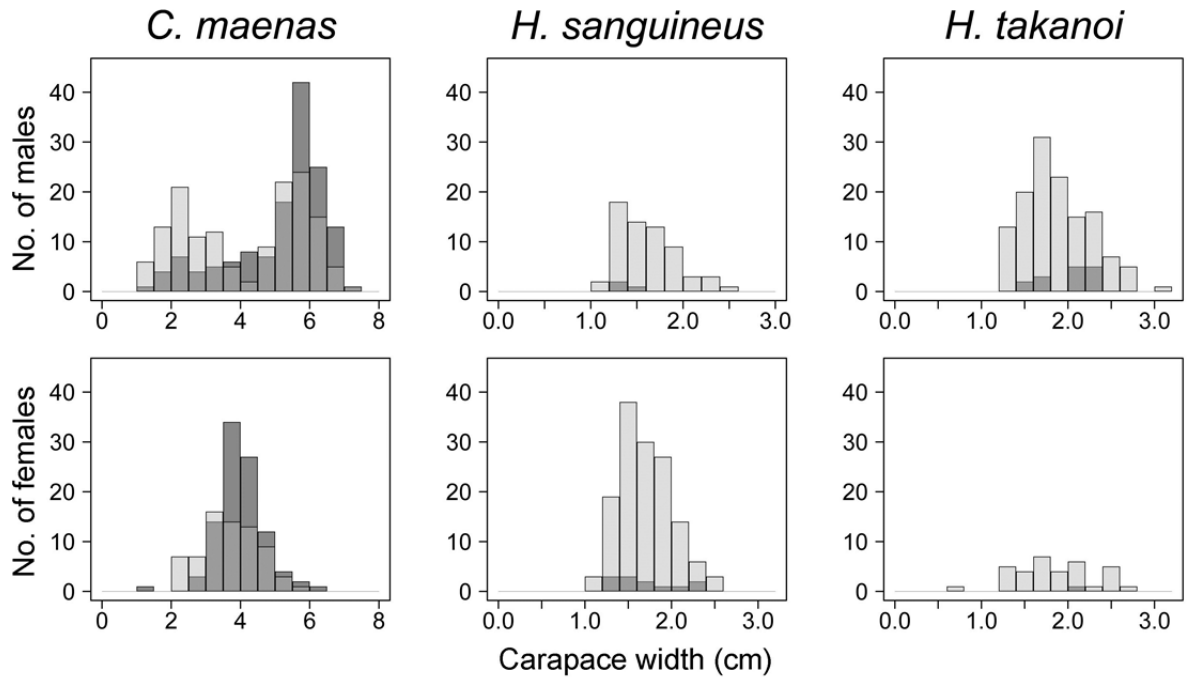


Figure S3. Frequency distribution of crab host sizes of the three crab species (*Carcinus maenas*, *Hemigrapsus sanguineus*, *Hemigrapsus takanoi*) separated into males (above) and females (below), with dark grey bars indicating crabs infected with acanthocephalans and in a transparent light grey layer on top the numbers of uninfected crabs. Both uninfected and infected crabs had sometimes overlapping sizes, resulting in intermediate grey bars. For sample sizes see Table 1.

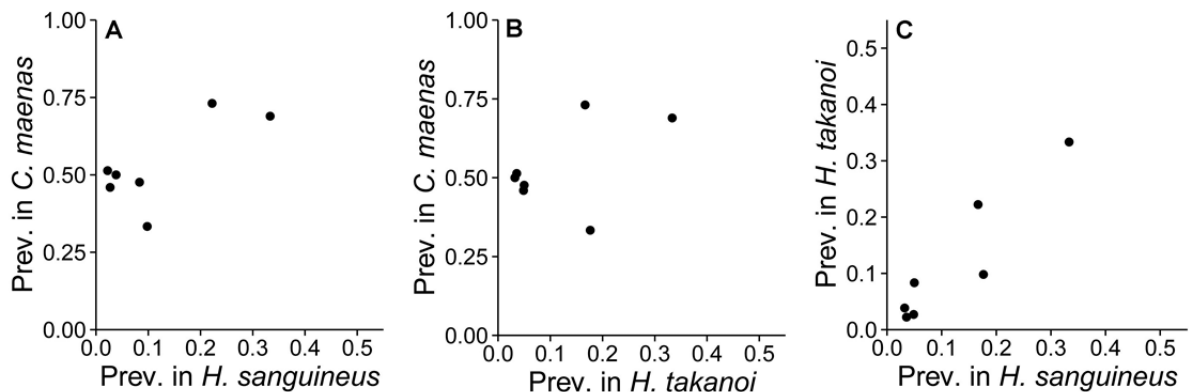


Figure S4. Correlations of prevalences of acanthocephalan infections at 7 sampling locations between A) *Carcinus maenas* and *Hemigrapsus sanguineus*, B) *C. maenas* and *Hemigrapsus takanoi*, and C) *H. takanoi* and *H. sanguineus*. For sample sizes see Table 1.

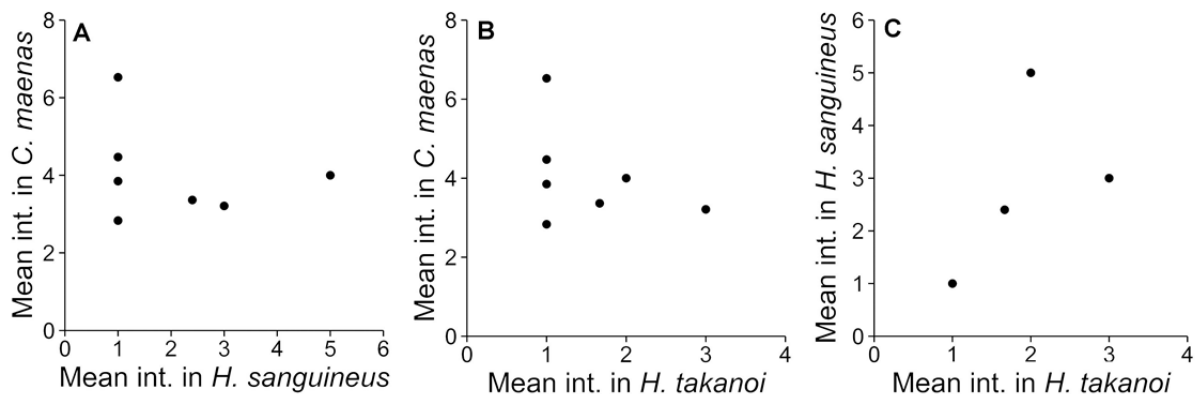


Figure S5. Correlations of mean intensities of acanthocephalan infections at 7 sampling locations between A) *Carcinus maenas* and *Hemigrapsus sanguineus*, B) *C. maenas* and *Hemigrapsus takanoi*, and C) *H. takanoi* and *H. sanguineus*. In this figure four locations had a mean intensity of 1 for both introduced crab species.

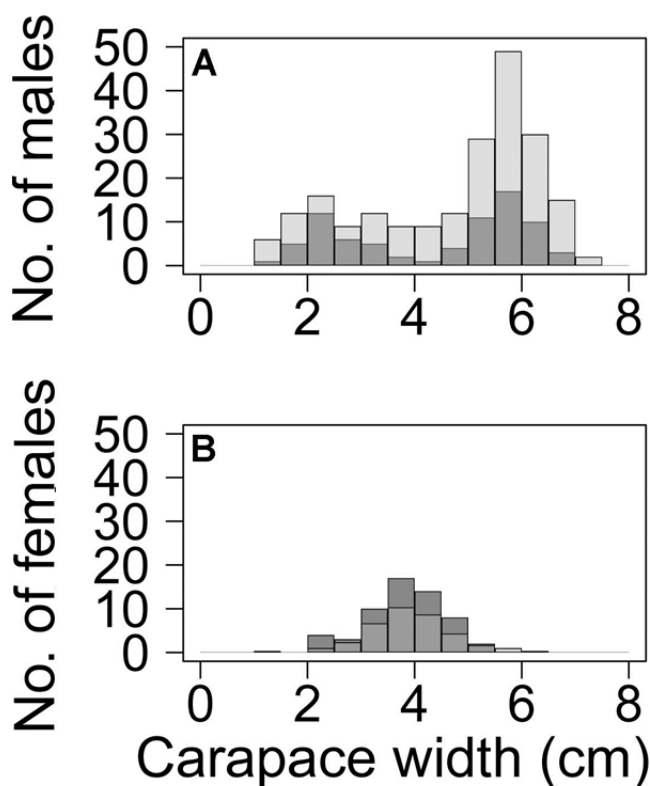


Figure S6. Frequency distribution of *Carcinus maenas* carapace sizes separated into males (A) and females (B), with dark grey bars indicating crabs infected with trematodes and in a transparent light grey layer on top the numbers of uninfected crabs. Both uninfected and infected crabs had sometimes overlapping sizes, resulting in intermediate grey bars. For sample sizes see Table 1.

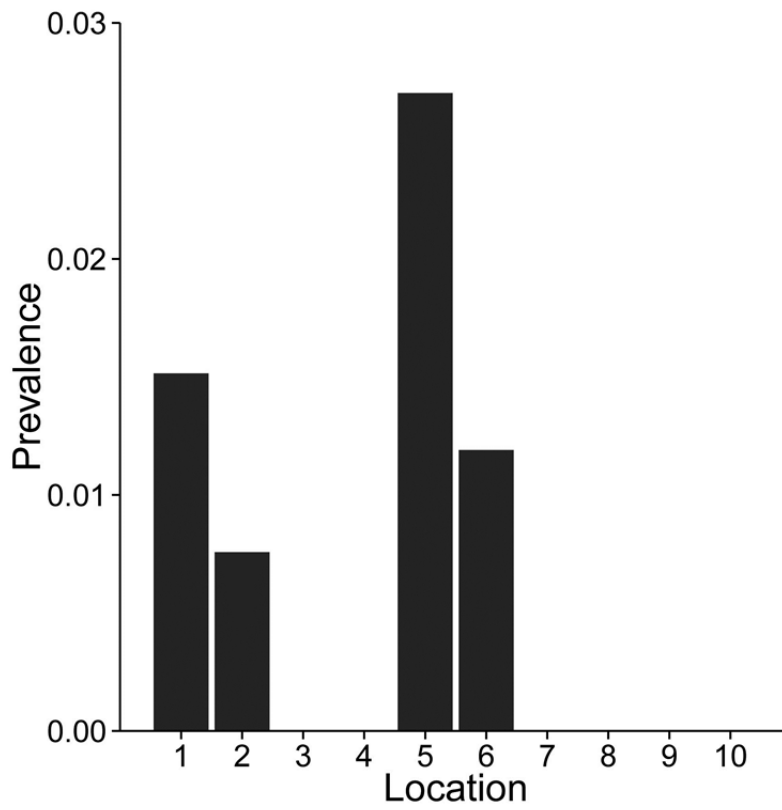


Figure S7. Prevalence of the rhizocephalan *Sacculina carcini* in *Carcinus maenas* crab hosts at the 10 sampling locations. For sample sizes see Table 1.